

Atomically dispersed Fe-O₄-C sites as efficient electrocatalysts for electrosynthesis of hydrogen peroxide

Liuyue Cao,^{a,f} Hongrui Wang,^a Ningyan Cheng,^{*c} Lei Zhang,^d Meiqing Shi,^{*e} Bin-Wei Zhang,^{*a,b}

^a School of Chemistry and Chemical Engineering, Chongqing University, Chongqing 400044, China.
E-mail: binwei@cqu.edu.cn

^b Center of Advanced Electrochemical Energy, Institute of Advanced Interdisciplinary Studies, Chongqing University, Chongqing 400044, China.

Key Laboratory of Structure and Functional Regulation of Hybrid Materials of Ministry of Education,

^c Key Laboratory of Structure and Functional Regulation of Hybrid Materials of Ministry of Education, Institutes of Physical Science and Information Technology, Anhui University, Hefei 230601, Anhui, China. E-mail: ningyancheng@ahu.edu.cn.

^d Centre for Clean Environment and Energy, Gold Coast Campus, Griffith University, Gold Coast, Queensland, 4222, Australia.

^e School of Metallurgy and Environment, Central South University, Changsha, Hunan 410083, China.
E-mail: shimeiqing0925@126.com

^f School of Chemical Engineering, University of New South Wales, 2 High Street, Kensington, Sydney, NSW, 2052, Australia.

Methods

Synthesis of SA Fe/GO samples. SA Fe/GO was synthesized via the dispersion of 6.0 mg FeCl_3 and 50 mg graphene oxide (GO) in Millipore water ($18.2 \text{ M}\Omega \cdot \text{cm}$) under ultrasonication for 30 min. The mixture was freeze-dried for 24 h to remove water, followed by thermal treatment in 5 vol% H_2 in N_2 at $300 \text{ }^\circ\text{C}$ for 2 h to form Fe nanoparticles (Fe NPs/ GO). Fe NPs/ GO was leached in 1M HCl for 12 h, and then 1M HNO_3 for 12 h to remove Fe NPs, the obtained sample named as SA Fe/GO. For comparison, GO was prepared through the same procedure without the addition of FeCl_3 .

Structural characterization. XRD results were recorded by a powder XRD (GBC MMA diffractometer) with Cu $\text{K}\alpha$ radiation at the scan rate of 2° min^{-1} . The XAS results of Co K-edge were collected at an XAS station of the Beijing Synchrotron Radiation Facility. EXAFS fitting is applied through Athena and Artemis software.¹ Wavelet transformation (WT) is also employed using the software package developed by Funke and Chukalina using Morlet wavelet with $\kappa = 10$, $\sigma = 1$.^{2,3} The morphological study of the newly developed catalysts was performed on an FEI Titan Themis Z microscope equipped with probe and image correctors at 300 kV.

Electrochemical measurements. The electrochemical performance of the resultant catalysts were carried out by using a three electrode system at an electrochemical workstation (CHI 760 E, CH Instrument, USA). A Pt wire was used as the counter electrode and a saturated calomel electrode was applied as the reference electrode. The working electrode was using a rotating disk electrode (RRDE). The ring electrode was Pt ring with an outside diameter of 0.75 mm and inside diameter of 6.5 mm; the disk electrode was a glass carbon disk with the diameter of 5.0 mm. The slurry was prepared by adding 5.0 mg catalysts into a mixture of 50 μL Nafion and 950 μL ethanol, and then was sonicated for 1 h to form a homogenous dispersion. 5 μL of the ink was dropped on the disk electrode. All the tests were carried out in a O_2 saturated 0.1 M KOH solution at room temperature with a rotated rate of 1600 rpm. Linear sweep voltammetry (LSV) was performed at a scan speed of 10 mV/s, and the potential of ring electrode was set at 1.2 V (vs. RHE) to detect the production of H_2O_2 . The potential (1.2 V vs. RHE) of the ring is set such that it can oxidize the H_2O_2 produced at the disk electrode, with the resulting current providing a measurement of the level of H_2O_2 . In this potential, the Pt ring may be surface oxidized, and it can be readily recovered by rapid cyclic voltammetry at low potentials to reduce PtO_x .

The potential was calibrated to a reversible hydrogen electrode (RHE) by applied the following equation:

$$E \text{ (RHE)} = E \text{ (SCE)} + 0.224 \text{ V} + 0.0592 \text{ pH}$$

The selectivity, production and electron transfer number were calculated by the following equations:

$$\text{H}_2\text{O}_2 \text{ selectivity: } \text{H}_2\text{O}_2 \text{ (\%)} = 200 \times (i_r/N) / (i_d + i_r/N)$$

$$\text{H}_2\text{O}_2 \text{ productivity (mg cm}^{-2} \text{ h}^{-1}) = \frac{1}{2} \times (i_r/N) \times M_{\text{H}_2\text{O}_2} \times 3600 / (F/A)$$

$$\text{electron transfer number (n)} = \frac{4 i_r}{i_r + i_d/N}$$

i_r was the ring current and i_d was the disk current, N is the current collection efficiency of Pt ring electrode ($N = 0.26$), $M_{\text{H}_2\text{O}_2}$ is the molecular weight of H_2O_2 ($M_{\text{H}_2\text{O}_2} = 34.01 \text{ g mol}^{-1}$), F is Faraday constant ($F = 96485.3 \text{ C mol}^{-1}$), A is the area of disk electrode ($A = 0.196 \text{ cm}^2$). The collection efficiency of the electrode defined as the fraction of product from the disk to the ring is 0.26.

The stability test of these catalysts was performed by the chronoamperometric at a constant potential of -1.2 V (vs. RHE).

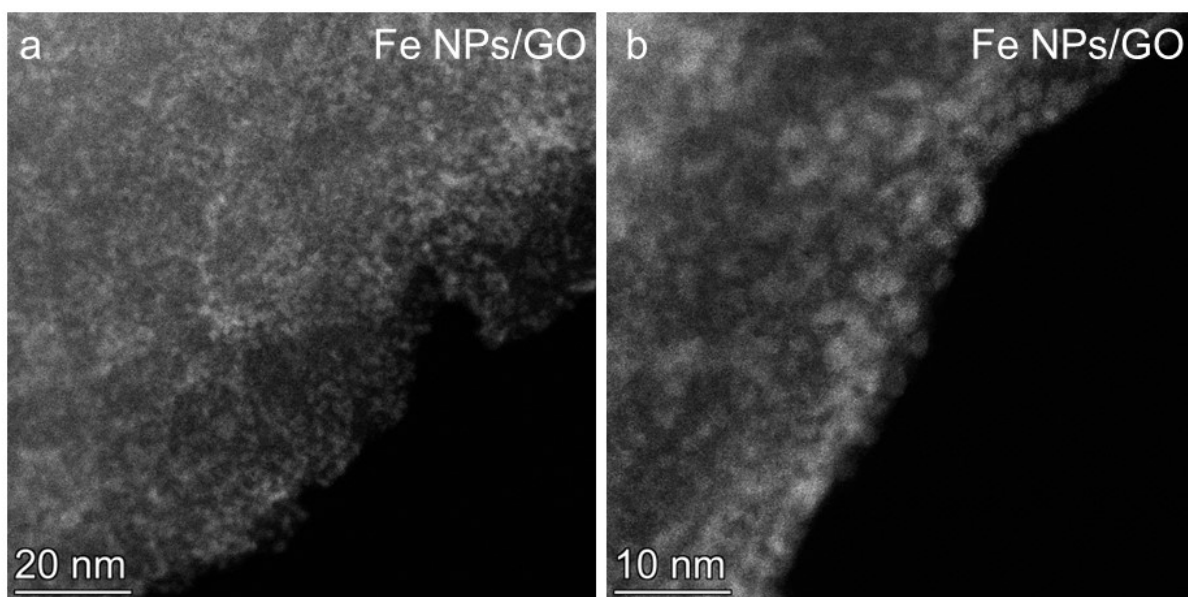


Figure S1. a-b, HAADF-STEM images of Fe NPs/GO.

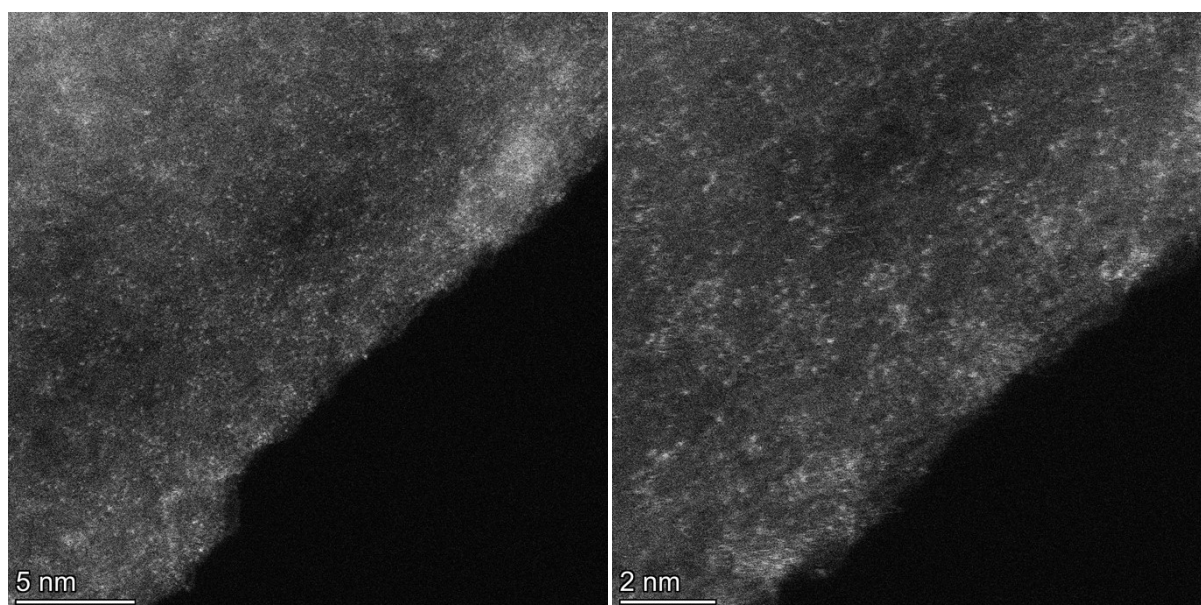


Figure S2. a-b, HAADF-STEM images of SA Fe/GO.

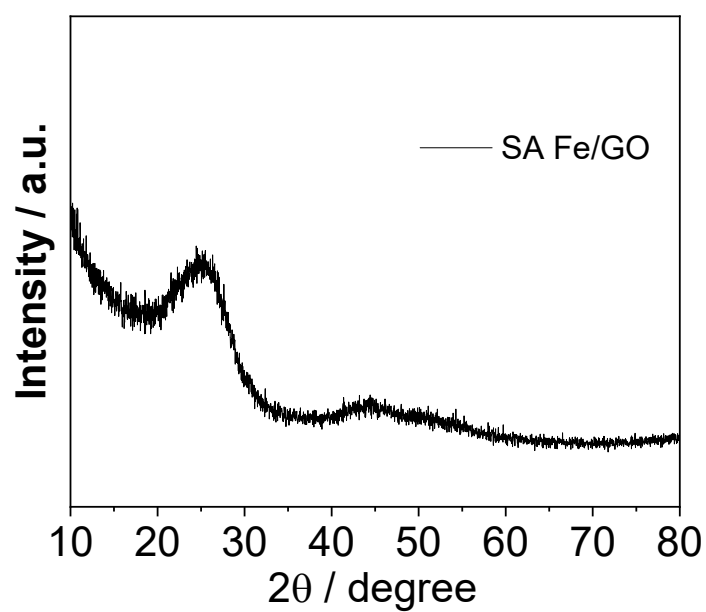


Figure S3. XRD patterns of the SA Fe/GO.

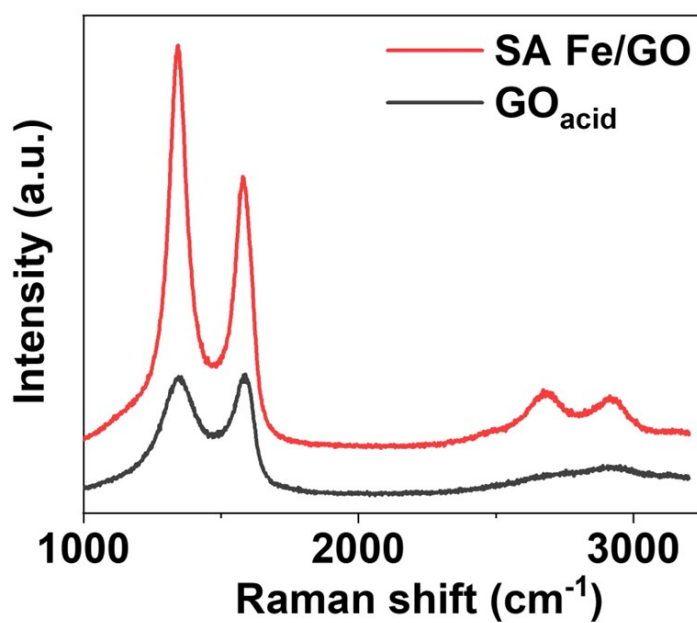


Figure S4. Raman spectra of GO_{acid} and SA Fe/GO.

Table S1. Fitting parameters for Fe K-edge EXAFS for the sample.

S_0^2 was obtained from Fe foil and fixed as 0.98. ΔE_0 was returned a value of -0.7780 ± 0.4972 eV. Data ranges $3.0 \leq k \leq 10.5 \text{ \AA}^{-1}$, $1.0 \leq R \leq 2.0 \text{ \AA}$. The number of variable parameters is 2, out of a total of 4.6563 independent data points, R factor for this fit is 1.08%. The Debye-Waller and ΔR are based on *guessing* parameters and fixed as 0.004 and 0.047.

Paths	CN	R	σ^2
Fe-O	4.2±0.2	2.03	0.004

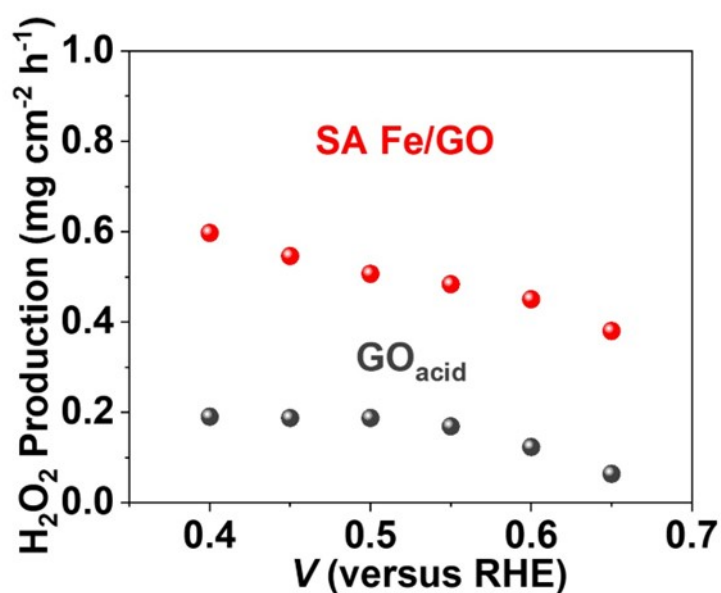


Figure S5. Electrosynthesis of H₂O₂ on GO_{acid} and SA Fe/GO in O₂-saturated 0.10 M KOH electrolyte.

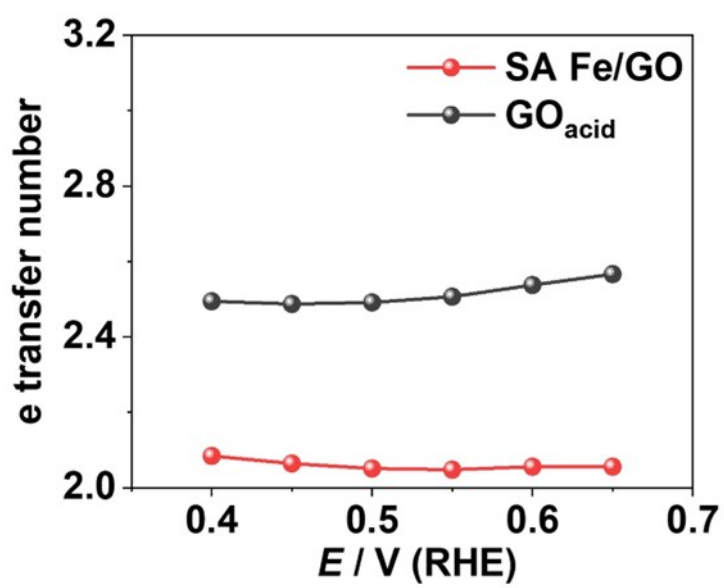


Figure S6. Calculated H_2O_2 electron transfer number during the potential sweep.

Table S2. Electrochemical performance comparison of the SA Fe/GO and other reported electrocatalysts for H₂O₂ electrochemical synthesis in alkaline environment.

Sample	Onset potential (RHE)	Selectivity	Electrolyte	Reference
SA Fe/GO	0.90 V	97% @0.6V	0.1 M KOH	This work
Pt-SA/rGO	0.96 V	90% @0.6V	0.1 M KOH	4
Co ₁ @NG(O)	0.8 V	72% @0.6 V	0.1 M KOH	5
Fe-CNT	0.82 V	94% @0.6 V	0.1 M KOH	6
Co-POC-O	0.84 V	81% @0.6 V	0.1 M KOH	7
Co ₁ @GO	0.91 V	81.4% @0.6 V	0.1 M KOH	8
Mo ₁ /OSG-H	0.78 V	95% @0.6 V	0.1 M KOH	9
O-CNT	0.77 V	90% 0.6V	0.1 M KOH	10
Meso C	0.75 V	78% @0.6 V	0.1 M KOH	11
N-CNF/Ni	0.78 V	70% @0.6 V	0.5 M KOH	12
CoSe ₂ NS/CC	0.72 V	90% 0.6 V	0.1 M KOH	13
cCTN:Cl ⁻	0.7 V	85% 0.6V	0.1 M KOH	14
Fe ₃ O ₄ / graphene	0.702 V	70% @0.6 V	1 M KOH	15

References

1. B. Ravel and M. Newville, *Journal of Synchrotron Radiation*, 2005, **12**, 537-541.
2. Z. Xia, H. Zhang, K. Shen, Y. Qu and Z. Jiang, *Physica B: Condensed Matter*, 2018, **542**, 12-19.
3. H. Funke, M. Chukalina and A. C. Scheinost, *Journal of Synchrotron Radiation*, 2007, **14**, 426-432.
4. X. Song, N. Li, H. Zhang, H. Wang, L. Wang and Z. Bian, *Journal of Power Sources*, 2019, **435**, 226771.
5. E. Jung, H. Shin, B.-H. Lee, V. Efremov, S. Lee, H. S. Lee, J. Kim, W. Hooch Antink, S. Park, K.-S. Lee, S.-P. Cho, J. S. Yoo, Y.-E. Sung and T. Hyeon, *Nature Materials*, 2020, **19**, 436-442.
6. K. Jiang, S. Back, A. J. Akey, C. Xia, Y. Hu, W. Liang, D. Schaak, E. Stavitski, J. K. Nørskov, S. Siahrostami and H. Wang, *Nature communications*, 2019, **10**, 3997.
7. B.-Q. Li, C.-X. Zhao, J.-N. Liu and Q. Zhang, *Advanced Materials*, 2019, **0**, 1808173.
8. B.-W. Zhang, T. Zheng, Y.-X. Wang, Y. Du, S.-Q. Chu, Z. Xia, R. Amal, S.-X. Dou and L. Dai, *Communications Chemistry*, 2022, **5**, 43.
9. C. Tang, Y. Jiao, B. Shi, J.-N. Liu, Z. Xie, X. Chen, Q. Zhang and S.-Z. Qiao, *Angewandte Chemie International Edition*, 2020, **59**, 9171-9176.
10. Z. Lu, G. Chen, S. Siahrostami, Z. Chen, K. Liu, J. Xie, L. Liao, T. Wu, D. Lin, Y. Liu, T. F. Jaramillo, J. K. Nørskov and Y. Cui, *Nature Catalysis*, 2018, **1**, 156-162.
11. S. Chen, Z. Chen, S. Siahrostami, T. R. Kim, D. Nordlund, D. Sokaras, S. Nowak, J. W. F. To, D. Higgins, R. Sinclair, J. K. Nørskov, T. F. Jaramillo and Z. Bao, *ACS Sustainable Chemistry & Engineering*, 2018, **6**, 311-317.
12. M. E. M. Buan, N. Muthuswamy, J. C. Walmsley, D. Chen and M. Rønning, *Carbon*, 2016, **101**, 191-202.
13. Y. Ji, Y. Liu, B.-W. Zhang, Z. Xu, X. Qi, X. Xu, L. Ren, Y. Du, J. Zhong and S. X. Dou, *Journal of Materials Chemistry A*, 2021, **9**, 21340-21346.
14. L.-Z. Peng, P. Liu, Q.-Q. Cheng, W.-J. Hu, Y. A. Liu, J.-S. Li, B. Jiang, X.-S. Jia, H. Yang and K. Wen, *Chemical Communications*, 2018, **54**, 4433-4436.
15. W. R. P. Barros, Q. Wei, G. Zhang, S. Sun, M. R. V. Lanza and A. C. Tavares, *Electrochim. Acta*, 2015, **162**, 263-270.